Surface Science 751 (2025) 122608

Contents lists available at ScienceDirect

Surface Science

journal homepage: www.elsevier.com/locate/susc

Growth and Ag-encapsulation of Pt islands on Ag(111) at room temperature

Buddhika S.A. Gedara, Michael Trenary *

Department of Chemistry, University of Illinois Chicago, 845 West Taylor Street, Chicago, IL 60607, United States

ARTICLE INFO

Keywords:
Scanning tunneling microscopy
Two-dimensional island nucleation and growth
Silver
Encapsulation of platinum islands
Platinum deposition on Ag(111)

ABSTRACT

The growth of Pt islands at submonolayer coverages on Ag(111) at room temperature were investigated with scanning tunneling microscopy. A two-step mechanism for growth of the islands is proposed. First, Pt replaces Ag substrate atoms through a place-exchange process. Next, Pt adatoms nucleate at substitutional Pt sites and Pt islands subsequently grow from these sites. At room temperature, Ag atoms migrate to cover Pt islands, creating vacancy pits on the terraces and bays on the step edges. Ag atoms nucleate at corner sites of the Pt islands, and the layer of Ag atoms on the Pt islands grow from these sites.

1. Introduction

Bimetallic catalysts often offer advantages over single metal catalysts as the composition can be adjusted to enhance activity and selectivity in important industrial reactions, such as hydrogenation. It is crucial to understand the atomic-level structure of bimetallic catalysts to enhance their performance. Although scanning tunneling microscopy (STM) has been used for decades to characterize the structures formed when one metal is deposited onto the surface of another, each combination is unique and requires separate study. Here we focus on Pt/Ag(111), which is relevant to the use of PtAg bimetallic catalysts for such processes as formate oxidation and hydrogen evolution [1], electrocatalysis and biosensing [2], the oxygen reduction reaction [3], and formic acid oxidation [4].

O'Connor et al. [5] reported that Pd islands on Ag(111) have the ability to dissociate H_2 molecules and the resulting H atoms can then move to and occupy Ag sites. Since Pt is also very active for H_2 dissociation, it is important to understand the atomic level behavior of Pt islands on Ag(111). Patel et al. [6] have studied the surface structure of 0.01 monolayer (ML) of Pt on Ag(111) as a function of deposition temperature with low temperature scanning tunneling microscopy (LT-STM). They discovered that a higher concentration of Pt atoms formed near Ag steps and that the Pt atoms are exchanged into the Ag terraces with increasing temperature. Furthermore, they found that CO binds more weakly to the Pt atoms embedded in the topmost atomic plane of the Ag(111) surface than to Pt(111).

While Ag on Pt(111) has been thoroughly examined in previous studies [7–11], we have used STM to study the growth of Pt islands with increasing submonolayer Pt coverages on Ag(111) to investigate aspects of this system that have not been previously addressed. We contrast the behavior with what we recently reported for Pd on the Ag(111) and Au (111) surfaces [12,13]. We find that the growth of Pt islands on Ag(111) can be explained through a two-step mechanism. First, Pt substitutes into the Ag substrate through place-exchange. Second, the substituted Pt atoms serve as nucleation sites for additional Pt atoms so that Pt-island growth occurs at these sites. Despite some similarities between Pd and Pt, such as higher surface free energies than Ag (Pd: 2.0 J m^{-2}; Pt: 2.7 J m^{-2}; Ag: 1.3 J m^{-2}) [14] and Pt having a lower lattice mismatch with Ag than Pd (Pd(Pt): ~4.8 % (~4.3 %)), we have observed significant differences in surface-alloy formation between Pt and Pd at room temperature, such as different moiré patterns on Pt islands and bay formation at the Ag(111) step edge upon Pt deposition. In addition to a 35 % higher surface free energy, the cohesive energy for Pt of 564 kJ/mol is 50 % higher than the 376 kJ/mol value for Pd [15]. A comparison of the enthalpies of mixing in the Ag-Pt and Ag-Pd solid systems shows very different values for Pt and Pd [16]. It is negative over the entire composition range for Ag-Pd, but positive for compositions above 25 % Ag in the Ag-Pt system, and only slightly negative for <25 % Ag. Although the implications of these differences in bulk properties for the behavior of Pt and Pd on the Ag(111) surface are not clear, they do imply that Pt and Pd might behave quite differently. It is also important to note that the structures observed after Pt deposition at room temperature are governed by the kinetics of various processes rather than by thermodynamics.

* Corresponding author.
E-mail address: mtrenary@uic.edu (M. Trenary).

https://doi.org/10.1016/j.susc.2024.122608
Received 29 May 2024; Received in revised form 27 July 2024; Accepted 9 September 2024
Available online 12 September 2024

2. Experimental

The experiments were carried out in an ultrahigh vacuum chamber (UHV) with a base pressure of 1×10^{-10} mbar and the STM images were obtained at room temperature with an Omicron variable-temperature scanning probe microscope (VT-SPM) system. All images are topographic and were acquired with Omicron MATRIX control electronics and software. The data was processed with the WSxM program provided by Nanotech [17]. The Ag(111) surface was cleaned by repeated cycles of sputtering with argon (3×10^{-5} mbar) and annealing to ~700 K. The surface was considered well-ordered and clean when a sharp (1×1) low energy electron diffraction (LEED) pattern and STM images with flat featureless terraces separated by monatomic steps were obtained. Pt was deposited on Ag(111) via evaporation from a pure Pt rod (GoodFellow, 99.95 %) by a triple electron beam evaporator (EFM 3T) with an integral flux monitor. The deposition rate for Pt was 6×10^{-4} ML/s. The Pt coverage was determined directly from the STM images and a coverage of 1 ML corresponds to one Pt atom per unit cell of the Ag(111) surface. During Pt evaporation, the Ag(111) crystal was held at room temperature and the background pressure never exceeded 3×10^{-10} mbar.

3. Results

(a) STM of Pt/Ag(111)

Fig. 1 shows STM images of 0.020±0.002 (a), 0.072±0.002 (b), and 0.140±0.010 (c) ML of Pt deposited on Ag(111) at room temperature. These coverage values represent averages from ~ 20 images of the same surface. At a coverage of 0.020 ML, Pt islands appear as randomly scattered bright dots. At a coverage of 0.140 ML, they form compact, irregularly shaped islands. As the coverage increases, both irregularly shaped compact Pt islands and bright dots can be observed. We found two different heights for the dots, 0.285 ± 0.014 and 0.083 ± 0.018 nm. Brune et al. [18] reported similar bright dots with a height of 0.29 nm, which they assigned to Ag dimers in the inverse system of Ag on Pt(111). However, they found that the dimers are stable only at $T \leq 110$ K, whereas we observed these bright dots at room temperature. Fig. 1d, e, and f show the island size distributions (s/<s>) corresponding to the STM images shown in Fig. 1a, b, and c, where s is the size of an island in terms of the surface area, which was measured using WSxM software, and ⟨s⟩ is the average island size at a given coverage. Such distributions can provide information on such things as the critical cluster size, i, needed for nucleating islands [19–21]. The critical island size depends not only on coverage, but also on temperature and flux. As Amar and Family note, $i + 1$ is the minimum number of atoms needed to form a stable island [21]. Thus, if the critical island size is a dimer, $i = 1$. For $i \geq 1$, the distributions peak at ⟨s⟩. If single atoms can act as nucleation sites, then $i = 0$, and a monotonically decreasing distribution occurs. The $i = 0$ case was invoked for Fe deposited onto Cu(100) at room temperature, where Fe atoms exchanged with Cu atoms to form immobile nucleation sites, with Fe island growth occurring about the Fe atoms embedded in the topmost Cu layer [22]. Island growth in heteroepitaxial systems following adatom embedding has been modelled in other cases as well [23–25]. The distributions in Fig. 1d, e, and f evolve from a simple monotonically decreasing form for 0.02 ML as expected for $i = 0$, to bidmodal forms for 0.072 and 0.140 ML with peaks for s/⟨s⟩ between 1 and 2. A bimodal distribution was observed in an STM study of Co deposited onto a Au(788) surface at 300 K, where the small islands were associated with Co nucleating at trap sites [26]. Fig. 2 shows the density of Pt islands vs. Pt coverage on Ag(111), which increases by only about 50 % as the coverage increases by more than a factor of six. This is consistent with island growth from already formed nucleation centers.

Fig. 3a shows a Pt island on Ag(111) with a measured height of 0.160 ±0.007 nm. Furthermore, the raised ring around the inside perimeter of the island has an apparent height above the rest of the island of ~0.04 nm. This kind of feature was reported by Bode et al. for Fe deposition on W(110) [27]. The 9.4 % larger lattice constant of W than of Fe leads to tensile stress in pseudomorphic growth. Bode et al. attributed this additional corrugation around the perimeter of the Fe islands to the movement of Fe atoms inwards, resulting in a reduction of the lattice

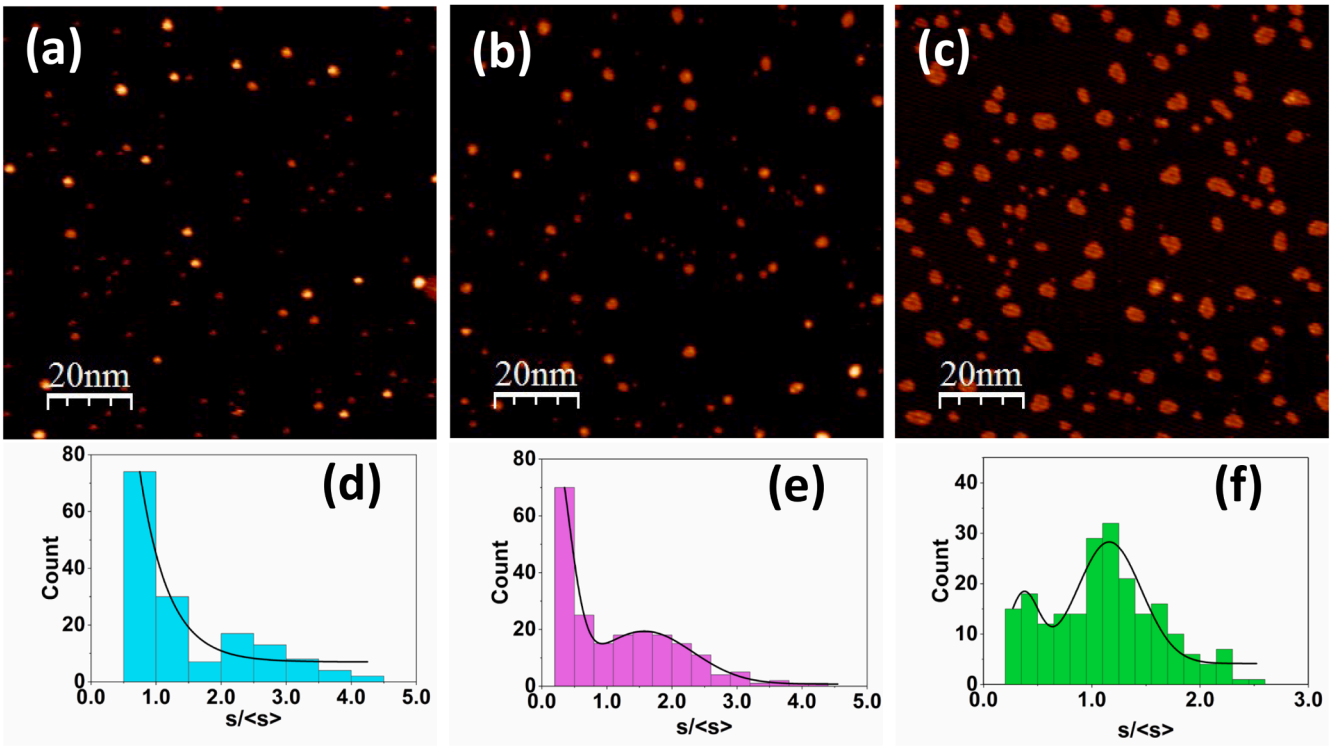

Fig. 1. STM images and corresponding Pt-island size distributions on Ag(111), at coverages of (a, d) 0.020 and (b, e) 0.072, and (c, f) 0.140 ML (scale, 100 × 100 nm^2). Image contrast was increased to clearly observe the Pt clusters and islands. Images were acquired at 0.20 nA, 1.0 V.

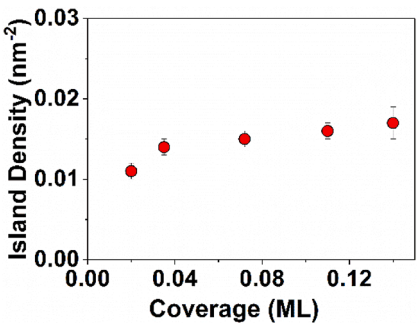

Fig. 2. Density of Pt islands vs. Pt coverage on Ag(111).

spacing to bring it closer to the bulk value of Fe [27]. The 4.3 % larger lattice constant of Ag than of Pt would also lead to tensile stress for pseudomorphic Pt islands on Ag(111). Thus, the relaxation at the perimeter of Pt islands on Ag(111) may lead to the additional corrugation of ~0.04 nm. The raised appearance at the perimeter of the Pt islands may also have an electronic contribution. This partial relaxation may hinder the coalescence of adjacent islands, as seen for Fe on W(110) [27]. This interpretation assumes that the first layer islands consist solely of Pt. Based on local work function measurements with STM, Patel et al. concluded that the Pt islands on Ag(111) consisted either entirely or mainly of Pt [6]. Nevertheless, we cannot rule out the possibility that some of the structure seen in the island shown in Fig. 3a is due to the incorporation of Ag atoms.

Previously, we reported that Pd atoms attach to ascending Ag step edges and can exchange with Ag atoms leading to Pd-rich brims on the upper terrace [12]. However, in the case of Pt deposition, we were unable to observe a distinct edge of Pt-rich brims on the Ag(111) upper terraces at room temperature. Nevertheless, Patel et al. reported Pt exchange with Ag atoms at the step edge for 0.01 ML of Pt deposition at 300, 380, and 480 K [6]. They noted that when the alloying temperature is increased to 380 K, Pt atoms are uniformly distributed, with minimal clumping of Pt clusters on the terraces. Additionally, wider borders containing a high concentration of Pt are formed above step edges, which are larger than those observed at a lower deposition temperature of 300 K [6].

Fig. 4a, b and c show bays (indentations) formed near the step edges upon Pt deposition. This bay formation was observed regardless of the Pt coverage. Since the Ag step edges are not decorated by Pt atoms, bay formation must be due to the removal of Ag atoms. The size of the bays increased with increasing Pt coverage. Brodde et al. [28] and Dulot et al. [29] reported erosion at the step edge upon Fe deposition on Cu(100) at room temperature. Furthermore, Dulot et al. reported that Cu(100) step edges are modified upon Fe deposition to act as Cu atom emitters, and these emitted Cu atoms can nucleate on the neighboring terraces [29]. Brodde et al. [28], Chang et al. [30], and Gilarowski et al. [31] also reported step roughening and surface etching upon deposition of Fe on Cu(100) at room temperature, Rh on Ag(100) at room temperature, and Ir on Cu(100) at 200 K, respectively. In the case of Rh/Ag(100), the experimental STM study [30] was followed by a Monte Carlo kinetics study of the surface etching mechanism [32].

(a) Ag migration and growth of vacancy pits at room temperature over time

The capping of Pt islands by Ag occurs at room temperature and produces islands that appear brighter than the uncapped Pt islands as shown in Figs. 5 and 6. The assumption that the brighter islands are Ag-capped is supported by the correlation of growth of the vacancy pits with increase in the number of brighter islands with time as seen in Fig. 6 and in the video in the supplementary materials. The heights of the Ag-covered Pt islands are 0.435 ± 0.008 nm. Patel et al. [6] reported a similar 0.459 nm height for Pt-rich islands capped by displaced Ag atoms upon place exchange after alloying at 300 K. In a previous study, we reported Ag- capped Pd islands with a height of 0.42 nm. Ag atoms migrated to the top of the Pd islands, nucleating at hexagonally-arranged defects located near the center of a Pd island [12]. In the case of Pt deposition, we observed in about 50 different STM images that Ag atoms nucleate at a particular feature (yellow circle in

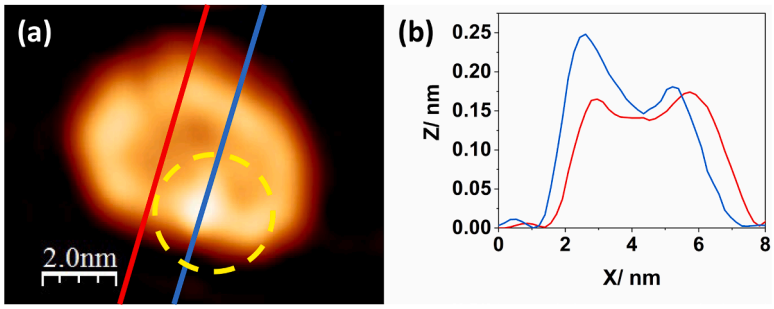

Fig. 3. (a) STM image of a Pt island showing the nucleation site (yellow circle) where Ag encapsulation of the island begins. Image was recorded at 0.2 nA, 1.0 V. (b) Height profile along red and blue lines of image in (a).

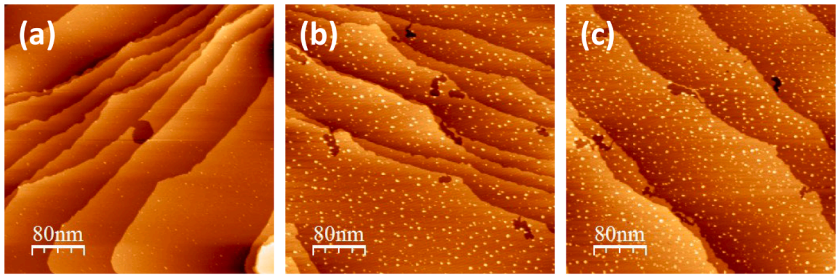

Fig. 4. STM images of (a) 0.020 and (b) 0.072, and (c) 0.140 ML of Pt on Ag (111) in a 400 × 400 nm^2 area. Bay formation at the step edges is observed at each coverage.

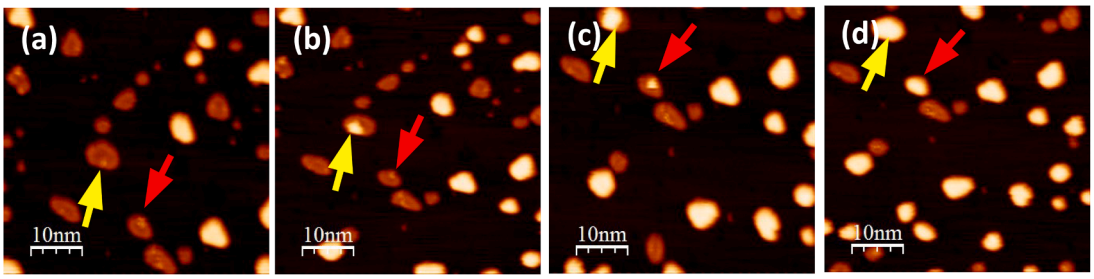

Fig. 5. STM images of 0.140 ML Pt/Ag(111) showing the migration of Ag atoms to the unique topographical feature on two Pt islands (yellow and red arrows). Images were recorded at 0.2 nA, 1 V. (a) $t = 0$, (b) $t = 4.8$ min, (c) $t = 12$ min, and (d) $t = 24$ min.

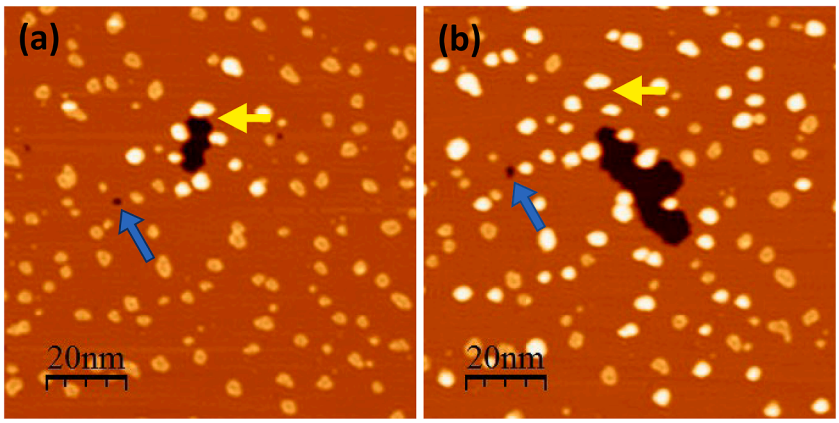

Fig. 6. Images in the same area showing the evolution of structure with time. (a,b) 0.140 ML of Pt deposited on the Ag surface at $t = 0$ s (a) and $t = 1$ hr 50 min (b). Yellow arrow shows the initial location of the vacancy pit and the blue arrow shows an isolated vacancy, which also moves, as shown by the video in the supplementary material. Images were recorded at 0.20 nA, 1.0 V.

Fig. 3) on the Pt islands. Patel et al. [6] identified these features as moiré patterns formed due to the lattice mismatch between Pt and the underlying Ag substrate. Fig. 6 shows how the 0.140 ML Pt/Ag(111) surface changes with time. The yellow arrows point to the same feature in images separated in time by 1 h 50 min. As the vacancy pit grew, its edge also shifted. Small, isolated vacancy pits were also observed, separate from the large vacancy pit, and these small vacancy pits moved around randomly. The video available in the supplementary materials shows the evolution from the structure of Fig. 6a to the structure of Fig. 6b.

4. Discussion

The structures observed with STM after depositing a low coverage of one metal onto the surface of another are largely determined by the kinetics of processes as the systems evolve to the equilibrium structures determined by thermodynamics. The higher surface free energies of both Pd and Pt compared to Ag imply that both Pt and Pd should eventually diffuse into the Ag bulk and this is indeed observed at higher temperatures. The structures observed here for low coverages of Pt deposited onto Ag(111) at room temperature are therefore metastable. The fact that the structures were observed to evolve on the time scale of minutes at room temperature reflects the dynamics of the processes. As we reported before, Pd atoms diffuse rapidly on Ag(111) terraces and as a result, the size of the Pd islands increases upon increasing the Pd coverage [12]. In contrast, Pt forms stable small clusters at a coverage of 0.020 ML and forms both stable small clusters and irregular islands at 0.140 ML. This difference between PdAg and PtAg may originate in differences in thermodynamic quantities [14–16] that lead to differences in the relevant kinetics. Patel et al. [6] reported the direct alloying of Pt with Ag terraces resulting in a more even dispersion of Pt atoms compared to Pd atoms throughout the Ag terraces. Direct alloying through place exchange appears to occur more readily for Pt than for Pd on Ag(111), and this is the main reason for their different island growth behavior.

Casari et al. [33] suggested that the substitution mechanism is primarily responsible for the formation of Pd islands on Au(111). They observed both place exchange between Pd and Au and adatom pinning in fcc/hcp hollow sites near the elbows in the herringbone reconstruction of the Au(111) surface. Furthermore, they reported that the pinning of Pd atoms on top of the sites that have undergone substitution serves as a trapping mechanism that is consistent with the observed growth dynamics [33]. Adatoms at these substituted sites are expected to have a higher binding energy than at unsubstituted sites. This results in the formation of the initial nucleus for island formation, and subsequent island growth is rapid as diffusing Pd atoms attach to existing islands. Meyer et al. have demonstrated that in heteroepitaxial growth of Ni on Ag(111), it is feasible for place-exchange to serve as a mechanism for creating sites for Ni adatom nucleation [24]. Meyer et al. [34] also studied Ni on Au(111) and reported a two-step mechanism for Ni island nucleation and growth. During the first step, Ni atoms exchange with the Au surface atoms, while in the second step, substitutional Ni atoms function as nucleation sites for Ni adatoms that diffuse across the surface [34]. Furthermore, they proposed that this mechanism applies broadly because Ni has a notably higher surface free energy and heat of sublimation than Au. Similarly, Pt has a higher surface free energy (2.7 J m^{-2}) and a higher heat of sublimation (cohesive energy) (564 kJ mol^{-1}) than Ag (1.3 J m^{-2}, 284 kJ mol^{-1}) [14,15]. This suggests that Pt/Ag (111) could follow the same two-step mechanism as Ni on Au(111). Similar conclusions were reached by Nouvertneét al. [35] in a study of Co on Cu(001) where at low coverages Co adatoms occupy substitutional sites in the Cu substrate surface and these sites act as pinning centers for subsequent island nucleation and growth.

Bay formation at the step edge and vacancy pit formation near the Pt islands were observed. Dulot et al. reported that inclusion of Fe into a Cu

(100) surface is responsible for the strong modification of the step edges [29]. Furthermore, the inclusion of Fe atoms introduces an elastic stress in the Cu(100) surface plane, and kinks and vacancy island formation is a possible channel for stress relaxation. The reduction of the barrier for atom detachment may also result from this stress, transforming Cu step atoms into a 2D adatom gas. This idea is consistent with our PtAg system and explains the bay formation near the step edge in Pt deposition. It will produce a Ag 2D adatom gas, and these Ag atoms nucleate at the special sites on the Pt islands to cover them.

At room temperature, Ag atoms migrated to cover the tops of the Pt islands without attaching to the perimeters of the islands to increase their lateral dimensions. The height of Ag encapsulated Pt islands is found to be 0.435±0.008 nm. Previously, we reported a dislocation-type structure on the Pd islands on Ag(111), providing nucleation sites for the growth of the second Ag layer, which began growing near the center of the Pd island [12]. However, such dislocation lines and defects are not evident on the Pt islands. Nevertheless, Patel et al. [6] have reported from LT-STM results that Pt islands on Ag(111) exhibit unique topographical features in the form of moiré patterns that relieve strain from the lattice mismatch. As shown in Fig. 3a (yellow circle) bright dots on the Pt islands are evident as was observed by Patel et al. [6] Since our Pt-island size is smaller than theirs, we were able to observe only one or two such dots per island. Furthermore, we found that growth of the second layer of Ag begins near these dots as shown in Fig. 5. We speculate that these dots correspond to Pt atoms out of registry with the Ag (111) lattice, making them more favorable binding sites for Ag atoms that migrate to the top of the Pt islands. In Fig. 6a, the Ag-capped Pt islands are clustered near the vacancy pit, but as the pit grows with time, capped islands are seen far from the pit in Fig. 6b. The growth of the pit, rather than formation of more pits, is explained by the fact that it requires less energy to enlarge a pre-existing pit compared to creating a new one. Additionally, the Ag atoms responsible for the growth of the capping layer may have come from detachment from steps or from Ag adatoms on the terraces. The energy barrier to pop-out a substrate atom next to a Pd island is less than at locations away from the Pd islands on Ag(111) [12,36]. This is presumably because as the Ag atoms break bonds to other Ag atoms, they begin to form bonds to the Pd atoms of the islands thereby lowering the energy of the process. Similarly, it is expected that the energy barrier to pop-out a Ag(111) substrate atom is also less next to a Pt island. Consequently, vacancy pits are readily formed on the Ag(111) terrace.

5. Summary and conclusions

The structures formed following deposition of low coverages of Pt on the Ag(111) surface at room temperature were studied with STM. Small clusters form at 0.020 ML of Pt, and both clusters and irregularly shaped compact islands emerge with increasing Pt coverage. The formation of Pt islands on Ag terraces occurs through a two-step mechanism. First, Pt replaces Ag substrate atoms. Second, additional Pt atoms bind more strongly to these substituted Pt atoms, which form the nucleation sites for island growth. The two-step mechanism is supported by the increase in Pt island density with coverage and the absence of a single peak in the island size distribution at $s/\langle s\rangle = 1$. There are two consequences of the higher surface free energy of Pt than Ag. First, migration of Pt atoms into the Ag bulk is thermodynamically favored and Pt islands remain on the surface indefinitely at room temperature only due to a high kinetic barrier for diffusion into the Ag bulk, which can be overcome at elevated temperatures. Second, Ag atoms diffuse to cover the Pt islands. Unique topographic features on the Pt islands provide nucleation sites for the growth of the second Ag layer. The Ag atoms needed to cover the Pt islands are generated by forming vacancy pits on the terraces and bays at the step edges of the Ag(111) substrate.

CRediT authorship contribution statement

Buddhika S.A. Gedara: Data curation, Investigation, Methodology, Validation, Writing – original draft. **Michael Trenary:** Writing – review & editing, Supervision, Project administration, Funding acquisition.

Declaration of competing interest

The authors declare that they have no known competing financial interests or personal relationships that could have appeared to influence the work reported in this paper.

Data availability

Data will be made available on request.

Acknowledgments

We thank Professor Nan Jiang for providing the Ag(111) single crystal. This work was supported by the National Science Foundation (CHE-2102622).

Supplementary materials

Supplementary material associated with this article can be found, in the online version, at doi:10.1016/j.susc.2024.122608.

References

[1] M. Huang, H. Zhang, S. Yin, X. Zhang, J. Wang, PtAg alloy nanoparticles embedded in polyaniline as electrocatalysts for formate oxidation and hydrogen evolution, ACS Appl. Nano Mater. 3 (2020) 3760–3766.
[2] C. Xu, Y. Liu, F. Su, A. Liu, H. Qiu, Nanoporous PtAg and PtCu alloys with hollow ligaments for enhanced electrocatalysis and glucose biosensing, Biosens. Bioelectron. 27 (2011) 160–166.
[3] X. Yang, L.T. Roling, M. Vara, A.O. Elnabawy, M. Zhao, Z.D. Hood, S. Bao, M. Mavrikakis, Y. Xia, Synthesis and characterization of Pt–Ag alloy nanocages with enhanced activity and durability toward oxygen reduction, Nano Lett. 16 (2016) 6644–6649.
[4] X. Jiang, X. Yan, W. Ren, Y. Jia, J. Chen, D. Sun, L. Xu, Y. Tang, Porous AgPt@Pt nanooctahedra as an efficient catalyst toward formic acid oxidation with predominant dehydrogenation pathway, ACS Appl. Mater. Interfaces 8 (2016) 31076–31082.
[5] C.R. O'Connor, K. Duanmu, D.A. Patel, E. Muramoto, M.A. van Spronsen, D. Stacchiola, E.C.H. Sykes, P. Sautet, R.J. Madix, C.M. Friend, Facilitating hydrogen atom migration via a dense phase on palladium islands to a surrounding silver surface, Proc. Natl. Acad. Sci. 117 (2020) 22657.
[6] D.A. Patel, P.L. Kress, L.A. Cramer, A.M. Larson, E.C.H. Sykes, Elucidating the composition of PtAg surface alloys with atomic-scale imaging and spectroscopy, J. Chem. Phys. 151 (2019) 164705.
[7] H. Röder, K. Bromann, H. Brune, K. Kern, Strain mediated two-dimensional growth kinetics in metal heteroepitaxy: Ag/Pt(111), Surf. Sci. 376 (1997) 13–31.
[8] H. Roder, R. Schuster, H. Brune, K. Kern, Monolayer-confined mixing at the Ag-Pt (111) interface, Phys. Rev. Lett. 71 (1993) 2086–2089.
[9] H. Brune, H. Röder, K. Bromann, K. Kern, Kinetic processes in metal epitaxy studied with variable temperature STM: Ag/Pt(111), Thin Solid Films 264 (1995) 230–235.
[10] H. Röder, H. Brune, J.-P. Bucher, K. Kern, Changing morphology of metallic monolayers via temperature controlled heteroepitaxial growth, Surf. Sci. 298 (1993) 121–126.
[11] M. Jankowski, E. van Vroonhoven, H. Wormeester, H.J.W. Zandvliet, B. Poelsema, Alloying, dealloying, and reentrant alloying in (sub)monolayer growth of Ag on Pt (111), J. Phys. Chem. C 121 (2017) 8353–8363.
[12] B.S.A. Gedara, M. Muir, A. Islam, D. Liu, M. Trenary, Room temperature migration of Ag atoms to cover Pd islands on Ag(111), J. Phys. Chem. C 125 (2021) 27828–27836.
[13] B.S.A. Gedara, M. Trenary, Stability of Pd islands on Ag(111) and Au(111), J. Phys. Chem. C 127 (2023) 516–522.
[14] L.Z. Mezey, J. Giber, The surface free energies of solid chemical elements: calculation from internal free enthalpies of atomization, Jpn. J. Appl. Phys. 21 (1982) 1569.
[15] C. Kittel, Introduction to Solid State Physics, John Wiley & Sons, Inc., Hoboken, NJ, 2005.
[16] I. Karakaya, W.T. Thompson, The Ag-Pt (Silver-Platinum) system, Bull. Alloy Phase Diagrams 8 (1987) 334–340.

[17] I. Horcas, R. Fernandez, J.M. Gomez-Rodriguez, J. Colchero, J. Gomez-Herrero, A. M. Baro, WSXM: a software for scanning probe microscopy and a tool for nanotechnology, Rev. Sci. Instrum. 78 (2007) 013705.
[18] H. Brune, H. Röder, C. Boragno, K. Kern, Microscopic view of nucleation on surfaces, Phys. Rev. Lett. 73 (1994) 1955–1958.
[19] H. Brune, G.S. Bales, J. Jacobsen, C. Boragno, K. Kern, Measuring surface diffusion from nucleation island densities, Phys. Rev. B 60 (1999) 5991–6006.
[20] J.W. Evans, P.A. Thiel, M.C. Bartelt, Morphological evolution during epitaxial thin film growth: formation of 2D islands and 3D mounds, Surf. Sci. Rep. 61 (2006) 1–128.
[21] J.G. Amar, F. Family, Critical cluster size: island morphology and size distribution in submonolayer epitaxial growth, Phys. Rev. Lett. 74 (1995) 2066–2069.
[22] D.D. Chambliss, K.E. Johnson, Nucleation with a critical cluster size of zero: submonolayer Fe inclusions in Cu(100), Phys. Rev. B 50 (1994) 5012–5015.
[23] A. Zangwill, E. Kaxiras, Submonolayer island growth with adatom exchange, Surf. Sci. 326 (1995) L483–L488.
[24] J.A. Meyer, R.J. Behm, Place-exchange as a mechanism for adlayer island nucleation during epitaxial growth and resulting scaling behavior, Surf. Sci. 322 (1995) L275–L280.
[25] D. Wang, Z. Wang, H. Zhu, Scaling of submonolayer island growth with reversible adatom exchange in surfactant-mediated epitaxy, Appl. Surf. Sci. 253 (2007) 8602–8606.
[26] V. Repain, S. Rohart, Y. Girard, A. Tejeda, S. Rousset, Building uniform and long-range ordered nanostructures on a surface by nucleation on a point defect array, J. Phys.: Condens. Matter 18 (2006) S17.
[27] M. Bode, R. Pascal, M. Dreyer, R. Wiesendanger, Nanostructural and local electronic properties of Fe/W(110) correlated by scanning tunneling spectroscopy, Phys. Rev. B 54 (1996) R8385–R8388.
[28] A. Brodde, H. Neddermeyer, Scanning tunneling microscopy on the growth of Fe films on Cu(100), Surf. Sci. 287-288 (1993) 988–994.
[29] F. Dulot, B. Kierren, D. Malterre, Influence of the initial step density on the growth mechanisms of the Fe/Cu(100) interface, Surf. Sci. 494 (2001) 229–237.
[30] S.L. Chang, J.M. Wen, P.A. Thiel, S. Günther, J.A. Meyer, R.J. Behm, Initial stages of metal encapsulation during epitaxial growth studied by STM: Rh/Ag(100), Phys. Rev. B 53 (1996) 13747–13752.
[31] G. Gilarowski, H. Niehus, Intermixing and Subsurface Alloy Formation: Ir on Cu (100), Surf. Sci. 436 (1999) 107–120.
[32] L.D. Roelofs, D.A. Chipkin, C.J. Rockwell, R.J. Behm, Mechanisms of hole formation in metal-on-metal epitaxial systems: Rh/Ag(001), Surf. Sci. 524 (2003) L89–L95.
[33] C.S. Casari, S. Foglio, F. Siviero, A.Li Bassi, M. Passoni, C.E. Bottani, Direct observation of the basic mechanisms of Pd island nucleation on Au(111), Phys. Rev. B 79 (2009) 195402.
[34] J.A. Meyer, I.D. Baikie, E. Kopatzki, R.J. Behm, Preferential island nucleation at the elbows of the Au(111) herringbone reconstruction through place exchange, Surf. Sci. 365 (1996) L647–L651.
[35] F. Nouvertné, U. May, M. Bamming, A. Rampe, U. Korte, G. Güntherodt, R. Pentcheva, M. Scheffler, Atomic exchange processes and bimodal initial growth of Co/Cu(001), Phys. Rev. B 60 (1999) 14382–14386.
[36] J.S. Lim, J. Vandermause, M.A. van Spronsen, A. Musaelian, Y. Xie, L. Sun, C. R. O'Connor, T. Egle, N. Molinari, J. Florian, K. Duanmu, R.J. Madix, P. Sautet, C. M. Friend, B. Kozinsky, Evolution of metastable structures at bimetallic surfaces from microscopy and machine-learning molecular dynamics, J. Am. Chem. Soc. 142 (2020) 15907–15916.